Carbon dioxide absorption by Ammonia-promoted aqueous triethanolamine solution in a packed bed

Hamed Rashidi[†], Hossein Azimi, and Parvaneh Rasouli

Chemical Engineering Department, Kermanshah University of Technology, Kermanshah, Iran

Abstract−CO_2 absorption by ammonia added triethanolamine aqueous solution as a promoter was investigated in terms of absorption percentage (AP), overall volumetric mass transfer coefficient (K_Ga_e), and molar flux (N_A) in a packed column. Three variables of ammonia concentration (0-5 wt%), Triethanolamine concentration (10-30 wt%), and gas flow rate (1,500-2,500 ml/min) were considered as significant variables in absorption performance. Effect of these variables and their interactions were inspected using the three level factorial response-surface method. Statistical analysis of the results showed that an ammonia concentration with 72.99%, 71.83, and 81.12% has the greatest effect on AP%, N_A, and K_Ga_e, respectively. Then, gas flow rate with 5.27% and 3.90%, had a great effect on AP% and K_Ga_e, respectively. Finally, the optimal operating conditions were determined to maximize the responses. Under optimal operating conditions, the maximum values for AP%, K_Ga_e, and N_A were 98.94%, 0.202 kmol/h·m³·kPa, and 3.901 kmol/m²·h, respectively. Thus, adding ammonia to triethanolamine considerably improves the mass transfer performance of solvent.

Keywords: Mass Transfer, Carbon Dioxide, Triethanolamine, Ammonia, Packed Bed

INTRODUCTION

The increase of CO_2 emission to the environment is of great worldwide concern, which leads to greenhouse effect and global warming [1]. Moreover, rise of greenhouse gases in the atmosphere causes environmental problems such as floods and sea level rise [2]. Carbon dioxide accounts for about 64% of greenhouse gases, so it has the greatest effect on global warming [3]. Thus, by controlling the CO_2 emission in the atmosphere, the earth's temperature can be controlled [4,5]. There are various methods for CO_2 capture, such as absorption, refrigeration, membrane, and adsorption (pressure swing adsorption and temperature swing adsorption) [6-8]. At present, the most common technology for CO_2 capture is absorption using different types of solvents, which are divided into two categories: 1) absorption using chemical solvents (chemical absorption) and 2) absorption using physical solvents (physical absorption). Rectisol and Selexol are physical solvents that have been widely used in many industrial processes [9]. At low temperature and high partial pressure of acid gases, the absorption process using physical solvents is preferable to the absorption process using chemical solvents. The advantage of the physical absorption process includes lower toxicity, lower vapor pressure, less corrosion, and more solvent stability. However, according to the low partial pressure of acidic gas in the post-combustion process, chemical absorption is usually used. Chemical absorption is the most complete technology for CO_2 capture. Most commercial units use this technology in the sweetening process [10]. There are many chemical solvents, such as alkanolamines, sodium hydroxide, ionic liquids, deep eutectic solvents, and

ammonia solution [11,12]. The use of alkanolamines is highly developed due to their availability, reasonable price, acceptable reaction rate, and high stability. Alkanolamines are divided into several groups: primary, secondary, and tertiary. Triethanolamine (TEA) and N-methyldiethanolamine (MDEA) are tertiary alkanolamines that are widely used due to their advantages over the primary and secondary amines [13]. One of their advantages is their reactive property. Unlike the primary and secondary alkanolamines, which react with CO_2 to form carbamate with high reaction heat and high energy consumption to regenerate of the absorbent, tertiary alkanolamines form bicarbonate with a low reaction heat and low regeneration energy. This means saving energy and reducing the operating costs of the acid gas removal unit. Furthermore, primary and secondary amines cause more corrosion than tertiary alkanolamines [14]. They evaporate quickly, causing a large loss of solvent and degradation in the presence of oxygen. However, tertiary amines reduce these problems despite their slower reaction rate with CO_2 [15]. According to the mentioned points, a promoter is needed to improve the absorption rate and reduce energy consumption. In this regard, developing a new amine absorbent by combining mentioned properties is necessary [16-18].

Singh et al. [19] studied the CO_2 absorption process using a mixture of TEA-monoethanolamine in a pack bed with recycle stream. Various operating parameters such as amine concentration, liquid flow and gas flow were used to evaluate the system behavior. Taguchi method was applied to determine the significance of parameters in the process.

Yeon et al. [20] investigated the absorption of carbon dioxide and the chemical reaction kinetics of CO_2 using a blend of TEA and piperazine (PZ) in a polyvinylidene fluoride hollow fiber membrane. Absorption was performed at temperature of 303 K to 382 K with PZ concentration of 0.26 M and 0.64 M, and TEA concentration

[†]To whom correspondence should be addressed.
E-mail: h_rashidi@kut.ac.ir

of 0.38 M, 1.13 M, and 2.26 M. The experimental results showed that the absorption capacity of the blend of TEA and PZ with CO_2 is mainly controlled by PZ, and adding PZ to TEA makes it possible to achieve high CO_2 removal efficiency. Finally, they examined the kinetic data for the reaction of PZ and CO_2 and calculated the activation energy through Arrhenius expression.

Compared with traditional amines, aqueous ammonia is a cheap solvent, has less corrosion and fewer degradation problems and can achieve high CO_2 removal capacity and absorbs items such as NO_X, SO_2 and CO_2 [21]. Praveen et al. [22] investigated the absorption of CO_2 by aqueous ammonia in a packed column. They studied the mass transfer coefficient in a wide range of operational variables. They found that in CO_2 absorption by aqueous ammonia, the mass transfer process is controlled by resistance in the liquid phase and the concentration of ammonia has a significant effect on the mass transfer coefficient. Generally, chemical solvents are not used individually in the CO_2 capture process. They are combined with additives that improve the absorbent performance and reduce problems such as corrosion, energy consumption, and erosion [16]. However, high vapor pressure of ammonia reduces efficiency of the CO_2 absorption process. Therefore, regarding the amine and ammonia solution absorbent, the main focus is on the pros and cons of a method that uses a mixture of these absorbents. Jeon et al. [23] added ammonia solution to MDEA and 2-amino-2-methyl-1-propanol (AMP) solutions to increase CO_2 uptake efficiency. The CO_2 uptake characteristics of ammonia added MDEA and AMP solutions were evaluated using a wetted wall column (WWC) and a packed column. Ammonia concentrations added to 30 wt% AMP and MDEA were 1-3 wt%. They found that the addition of NH_3 significantly increased the mass transfer performance of MDEA and AMP solutions due to the increase of free ammonia in the absorbent. They report that CO_2 uptake rate in AMP/NH_3 solution is higher than aqueous solution of MDEA/NH_3.

From the previous works, it can be said that no former study has been performed on CO_2 absorption by adding ammonia to TEA in a packed column. Due to the ability of ammonia to improve the rate of absorption and the ability of TEA to reduce vapor pressure of solution and ammonia loss, in this study, the mass transfer performance of TEA-NH_3 aqueous solution for CO_2 capture process was performed by using a packed column. Ammonia concentration, TEA concentration and gas flow rate were considered as operational variables. After determining the thermophysical properties of TEA-NH_3 aqueous solvent, effect of the mentioned variables and their interactions on AP%, K_Ga_e and N_A was investigated using the three level factorial response-surface method. Finally, the optimal operating conditions were determined to maximize the responses.

THEORY

1. Chemical Reactions

The CO_2 reacts with water to produce bicarbonate ion via CO_2 hydration reaction and the hydroxyl ion reaction, which are as follows:

$$CO_2 + H_2O \leftrightarrow HCO_3^- + H^+ \tag{1}$$

$$CO_2 + OH^- \leftrightarrow HCO_3^- \tag{2}$$
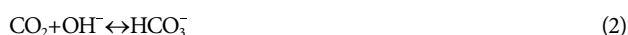
In contrast, the process of CO_2 hydration is so slow that it can be ignored, but hydroxyl ion reaction is rapid and is able to increase mass transfer even at low concentrations.

In general, the reaction between tertiary amines (R_3N) and carbon dioxide in aqueous solution can be expressed as follows:

$$CO_2 + R_3N + H_2O \leftrightarrow R_3NH^+ + HCO_3^- \tag{3}$$
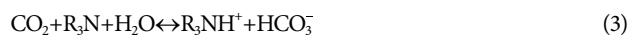
Triethanolamine (HO-CH_2-CH_2)$_2$-N-CH_2-CH_2-OH is a tertiary alkanolamine, where there is no hydrogen atom attached to the nitrogen atom in it. Therefore, it cannot react directly with CO_2 and acts only as a base catalyst for the formation of hydroxyl ion [24].
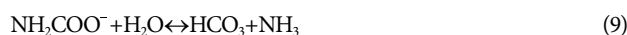
The following reactions occur from the interaction of aqueous ammonia and CO_2:

$$CO_2 + 2NH_3 \rightarrow NH_2COONH_4 \tag{4}$$

$$CO_2 + 2NH_3 + H_2O \leftrightarrow (NH_4)_2CO_3 \tag{5}$$

$$CO_2 + NH_3 + H_2O \leftrightarrow NH_4HCO_3 \tag{6}$$

Reaction (4) consists of the following reactions:

$$CO_2 + NH_3 \leftrightarrow NH_2COOH \tag{7}$$

$$NH_3 + NH_2COOH \leftrightarrow NH_4^+ + NH_2COO^- \tag{8}$$

Then, the hydrolyze reaction of NH_2COONH_4 occurs immediately and free ammonia is produced.

$$NH_2COO^- + H_2O \leftrightarrow HCO_3 + NH_3 \tag{9}$$

$$NH_3 + H_2O \leftrightarrow NH_3H_2O \tag{10}$$

Unlike reaction (7), which is a very fast reaction, reaction (8) is slow to affect the rate of the absorption directly. Finally, due to indirect reaction of TEA and CO_2, the reaction between ammonia promoted aqueous TEA solution is mainly controlled by reaction (7) [22].

2. Introducing the Responses

2-1. Absorption Percentage

To determine the CO_2 absorption percentage (AP), the molar ratio of CO_2 in the gas phase should be measured before and after passing through the packed column and applied in the following equation:

$$AP(\%) = \left(1 - \frac{Y_{out}}{Y_{in}}\right) \times 100 \tag{11}$$

Y_{in} and Y_{out} represent the molar ratios of CO_2 at the inlet and outlet of the absorption bed, respectively.

2-2. Overall Volumetric Mass Transfer Coefficient (K_Ga_e)

The relation proposed by Zeng et al. was used to calculate the overall volumetric mass transfer coefficient [25]:

$$K_Ga_e = \frac{F}{hP}\left[\ln\left(\frac{Y_{in}}{Y_{out}}\right) + (Y_{in} - Y_{out})\right] \tag{12}$$

where K_G, a_e, F, h, and P refer to the mass transfer coefficient (kmol/m^2·h·kPa), effective surface area (m^2/m^3), the inert gas flow rate (kmol/m^2·h), the height of absorption bed (m), and the pressure (kPa), respectively.

2-3. Volumetric Molar Flux (N_Aa_e)

The following equation has been employed to calculate the volumetric molar flux:

$$N_A a_e = \frac{F}{h}(Y_{in} - Y_{out}) \tag{13}$$

N_A is the molar flux (kmol/m^2·h), and a$_e$ is the effective surface area of gas-liquid (m^2/m^3). To calculate molar flux, effective surface area must be determined.

2-4. Effective Surface Area of Mass Transfer (a$_e$)

The relation used to determine the effective area is as follows [26]:

$$\frac{a_e}{a_p} = 3 \times \varepsilon^{0.5} \times Re^{-0.2} \times Fr^{-0.45} \times We^{0.75} \tag{14}$$

ε is the void fraction, a$_p$ is the specific area of the dry packing (m^2/m^3), Re is Reynolds number, Fr is Froude number, and We is Weber number. The dimensionless numbers of Reynolds, Weber, and Froude have definitions, which are discussed below:

$$Re_L = \frac{u_L}{a_P} \times \frac{\rho_L}{\mu_L} \tag{15}$$

$$Fr_L = \frac{u_L^2 \times a_P}{g} \tag{16}$$

$$We_L = \frac{u_L^2}{\delta_L} \times \frac{\rho_L}{a_P} \tag{17}$$

$$u_L = \frac{Q}{A} \tag{18}$$

In the above relations, Q, A, u$_L$, ρ_L, δ_L, g, and μ_L represent to the liquid volumetric flow rate (m^3/s), cross section area of tower (m^2), superficial velocity (m/s), density of the liquid (kg/m^3), surface tension of the liquid (N/m), gravitational constant (m/s^2) and viscosity of liquid (kg/m·s), respectively [27].

EXPERIMENTAL

1. Materials

The materials used in this study are aqueous ammonia (25%) purchased from Merck, TEA provided from Shazand Petrochemical Company and carbon dioxide supplied from Caspian Company.

2. Thermophysical Properties

Density, viscosity and surface tension are the thermophysical properties that play a significant role in the analysis of absorption and regeneration process. Hence, these thermophysical properties have been measured under various temperature and concentration for TEA-ammonia aqueous solution. The mentioned properties are also important for designing of CO$_2$ absorption column, modelling and designation of reaction rate constants [28]. The accuracy of the

Table 1. Thermophysical properties of TEA-NH$_3$ aqueous solution

TEA concentration (wt%)	NH$_3$ concentration (wt%)	Temperature (°C)	Density (g/cm^3)	Kinematic viscosity (mm^2/s)	Surface tension (mN/m)
10	0	20	1.0104	1.374	58.61
10	0	30	1.0098	1.039	56.16
10	0	40	1.0066	0.923	55.51
20	0	20	1.0270	1.958	57.42
20	0	30	1.0261	1.473	54.26
20	0	40	1.0220	1.278	53.93
30	0	20	1.0428	2.957	54.9
30	0	30	1.0421	2.231	52.4
30	0	40	1.0381	1.929	51.52
10	2.5	20	0.9945	1.456	57.23
10	2.5	30	0.9944	1.151	53.97
10	2.5	40	0.9905	0.983	53.44
20	2.5	20	1.0112	1.996	56.08
20	2.5	30	1.0106	1.640	53.64
20	2.5	40	1.0071	1.420	52.84
30	2.5	20	1.0265	3.020	54.11
30	2.5	30	1.0255	2.419	51.43
30	2.5	40	1.0216	1.968	51.07
10	5	20	0.9784	1.493	55.88
10	5	30	0.9783	1.210	53.54
10	5	40	0.9750	1.034	52.66
20	5	20	0.9939	2.152	55.06
20	5	30	0.9933	1.738	52.82
20	5	40	0.9900	1.487	52.19
30	5	20	1.0089	3.323	52.26
30	5	30	1.0084	2.588	50.93
30	5	40	1.0058	2.069	50.25

results, were confirmed by measuring the physical properties of pure water and aqueous TEA solution and comparing them with literature.

2-1. Density

A Gay-Lussac pycnometer with a capacity of 50 ml was employed to determine the density of TEA-ammonia solution with various concentration ranges at temperatures of 20, 30, and 40 °C. Note that to reduce the error in density measurement, each experiment was repeated three times and finally their mean value was collected in Table 1. According to the table, density decreases with increasing temperature and ammonia concentration increases with increasing TEA concentration.

2-2. Viscosity

The viscosity of the hybrid solvent of TEA-ammonia with different concentration ranges at temperatures of 20-40 °C was measured using capillary viscometer model C-100, NO.596, Cannon Fenske. The results of viscosity measurements are also presented in Table 1 and each value is the mean of three measurements. Pursuant to the table, it can be said that viscosity increases with increasing ammonia and TEA concentration and decreases with increasing temperature.

2-3. Surface Tension

The Kibron EZ-PI PlusTensiometer is used to determine the surface tension of a TEA-ammonia solvent with measuring range of 1-350 mN/m and accuracy/sensitivity of 0.01 mN/m. The results of surface tension measurements are in Table 1 and each value is the mean of three measurements. The reported numbers well indicate that surface tension decreases with increasing temperature, ammonia concentration and TEA concentration.

3. Setup and Methods

In this study, to experimentally measure of CO_2 absorption rate by a mixture of aqueous ammonia and TEA, a device that its schematic is shown in the Fig. 1, has been used.

All experiments were performed at atmospheric pressure, inlet solvent flow rate 40 ml/min, solvent inlet temperature 40 °C and, the inlet gas flow rate had different amounts of 1,500, 2,000 and 2,500 ml/min. The absorption tower consisted of a Plexiglass column with an inner diameter of 5 cm and a height of 50 cm that

40 cm from the length of the tower is filled by glass Raschig rings with a nominal size of 6 mm and 1 mm thickness. The surface area of the packing was 720 m^2/m^3 and free volume of 67%. Liquid inlet and gas outlet were located at the top of the tower and liquid outlet and gas inlet were at the bottom of the tower. The solution used in this experiment was made by mixing TEA and aqueous ammonia with the desired percentages. At the beginning of each experiment, the solution after reaching the desired temperature (40 °C) in reservoir is pumped to the absorption tower in a closed loop. Then, sufficient time is given to uniform the temperature of absorption tower and the solution. Note that all devices were insulated to prevent energy loss. After that, gas was introduced to the packed bed. In all experiments, feed gas contained 90 vol% of air and 10 vol% of carbon dioxide, which were mixed together before entering the tower and then passed through a humidifier for humidification. Different flow rates for inlet gas were considered during the tests; for this purpose, mass flow controllers (MFCs) were used to measure and regulate air and carbon dioxide gas. Subsequently, the solution and the gas stream flowed through the tower countercurrently. Exhaust gas from the top of the tower passed through the gas washing section, containing concentrated sulfuric acid, to eliminate ammonia and humidity. Finally, gas was passed through a sensor to measure the amount of carbon dioxide.

To select the upper and lower limit for experiments, at first, the hydrodynamics of packed bed was investigated by observing the differential pressure as a function of gas flow rate to determine the flooding point. Then, 70% flooding was considered for center point, 87% flooding for maximum gas flow and 50% for minimum. In the case of TEA concentration, preliminary CO_2 absorption experiments by aqueous TEA solution in the range of 10-60 wt% were conducted. Low absorption efficiency (lower than 40%) was observed. Moreover, higher TEA concentration (30-60 wt%) had negative effect on absorption efficiency. Therefore, 10-30 wt% was selected for TEA concentration. According to the literature, a low ammonia concentration (<5 wt%) was selected to reduce ammonia loss [23,29].

All experiments were repeated three times. The uncertainty analyses and device properties, such as flow meters, CO_2 sensors, and other controllers, are given in supplementary material. The accu-
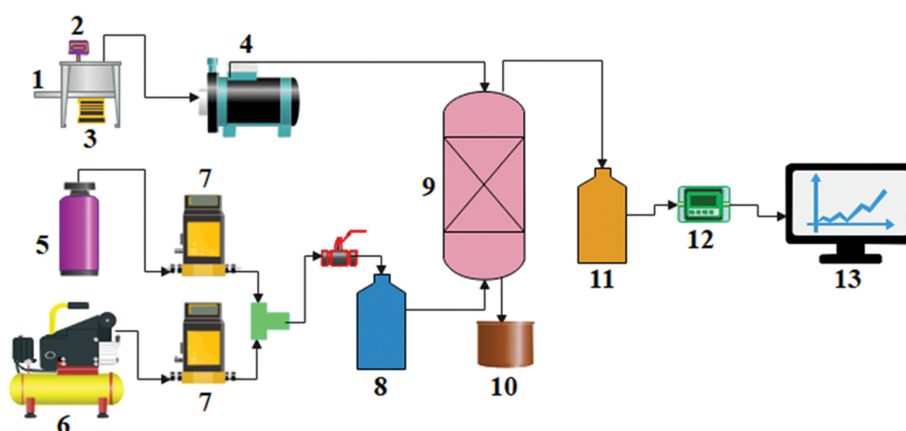

Fig. 1. Schematic of the device used for the absorption of carbon dioxide: 1) Reservoir containing solvent, 2) Temperature controller, 3) Heater, 4) Peristaltic pump, 5) CO_2 Cylinder, 6) Air compressor, 7) Mass flow controller, 8) Humidifier, 9) Packed bed, 10) Solvent tank, 11) Gas washing, 12) CO_2 sensor, 13) Recorder.

racy of the results was checked by measuring CO_2 loading of outlet liquid stream using the titration technique. The obtained mass balance error was less than 8.0%.

RESULT AND DISCUSSION

1. Design of Experiments

Design expert software and response surface three level factorial method were used to design experiments and statistical analysis of the results. Three variables of ammonia concentration, TEA concentration and gas flow were considered as effective variables on absorption performance. For each variable, three levels of minimum (1), middle (0) and maximum (+1) were defined. These variables and their values are listed in Table 2. In this study, CO_2 absorption performance by TEA-ammonia hybrid solvent was investigated in terms of absorption percentage (AP%), overall volumetric mass transfer coefficient (K_Ga_e) and molar flux (N_A). In Table 3, the experiments designed by the software (30 experiments with three replications at middle conditions) and response values are

Table 2. The operational variables and determined levels

Variables	Unit	Symbol	Levels		
			−1	0	+1
TEA concentration	wt%	A	10	20	30
NH_3 concentration	wt%	B	0	2.5	5
Gas flow	ml/min	C	1,500	2,000	2,500

presented. In the response surface method, there are many models, such as quadratic, mean, and linear, to predict the response. The quadratic model, which is known as the most complete and reliable model in the following form, was used:

$$Y = \beta_0 + \sum_{i=1}^{k} \beta_i X_i + \sum_{i=1}^{k} \beta_{ii} X_i^2 + \sum_{i=1}^{k-1} \sum_{j=1+i}^{k} \beta_{ij} X_i X_j \qquad (19)$$

where Y is the predicted output, X_i and X_j are the encoded values of variables. k is the number of variables. $X_i X_j$ and X_i^2 are terms related to the interactions and quadratic of variables, respectively.

Table 3. Experimental design and the obtained results

Std	Run	A: TEA Conc. (wt%)	B: NH_3 Conc. (wt%)	C: Gas flow rate (ml/min)	K_Ga_e (kmol/m³·h·kPa)	AP (%)	N_A (kmol/m²·h)
9	1	30	5	1,500	0.21	97.71	2.54
27	2	30	5	2,500	0.14	76.99	3.34
20	3	20	0	2,500	0.02	18.50	0.92
28	4	20	2.5	2,000	0.14	58.57	3.32
14	5	20	2.5	2,000	0.14	58.69	3.32
7	6	10	5	1,500	0.15	93.89	2.97
12	7	30	0	2,000	0.02	24.21	0.85
6	8	30	2.5	1,500	0.15	93.08	2.45
24	9	30	2.5	2,500	0.12	71.83	3.15
19	10	10	0	2,500	0.02	17.29	0.95
15	11	30	2.5	2,000	0.15	86.53	3.03
3	12	30	0	1,500	0.02	31.59	0.83
17	13	20	5	2,000	0.17	89.87	3.46
2	14	20	0	1,500	0.02	29.29	0.87
13	15	10	2.5	2,000	0.12	81.12	3.46
23	16	20	2.5	2,500	0.11	69.00	3.34
8	17	20	5	1,500	0.18	95.96	2.77
30	18	20	2.5	2,000	0.14	57.94	3.32
21	19	30	0	2,500	0.02	22.41	0.98
5	20	20	2.5	1,500	0.13	90.96	2.65
29	21	20	2.5	2,000	0.14	58.13	3.32
18	22	30	5	2,000	0.19	92.21	3.20
11	23	20	0	2,000	0.02	22.49	0.89
25	24	10	5	2,500	0.12	72.82	3.84
26	25	20	5	2,500	0.13	74.16	3.57
4	26	10	2.5	1,500	0.11	86.04	2.75
22	27	10	2.5	2,500	0.10	65.77	3.50
1	28	10	0	1,500	0.02	23.43	0.77
10	29	10	0	2,000	0.02	19.57	0.86
16	30	10	5	2,000	0.14	85.35	3.60

Table 4. ANOVA table for $K_G a_e$

Source	SS	DF	MS	F-value	P-value	
Model	0.1069	8	0.0134	287.89	0.0001>	Significant
A: C-TEA	0.0024	1	0.0024	53.34	0.0001>	
B: C-NH$_3$	0.0855	1	0.0855	1,842.14	0.0001>	
C: Gas flow	0.0023	1	0.0023	48.99	0.0001>	
AB	0.0008	1	0.0008	16.28	0.0006	
AC	0.0003	1	0.0003	5.88	0.0245	
BC	0.0020	1	0.0020	42.71	0.0001>	
B^2	0.0110	1	0.0110	237.39	0.0001>	
C^2	0.0011	1	0.0011	24.03	0.0001>	
Residual	0.0010	21	0.0000			
Lack of fit	0.0010	18	0.0001			
Cor total	0.1079	29				
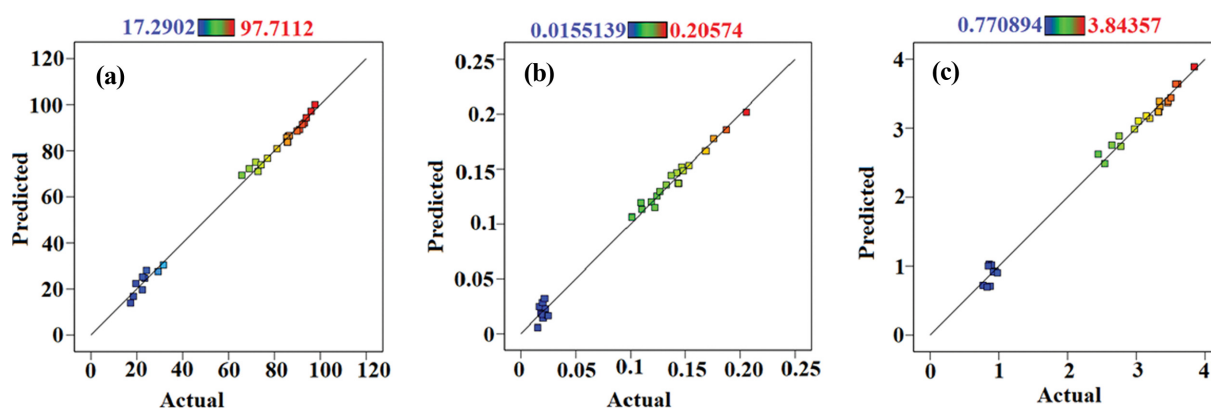
Fig. 2. Actual values versus predicted values for (a) AP, (b) $K_G a_e$, and (c) N_A.

β_0, β_i, β_{ii} and β_{ij} represent coefficients of constant, linear, quadratic, and interaction, respectively [30].

2. Statistical Analysis

To confirm the validity of the model in the prediction of AP, $K_G a_e$ and N_A, the predicted data were statistically analyzed. The accuracy and validity of the model in prediction of $K_G a_e$ can be checked by the analysis of variance (ANOVA) presented in Table 4. Accuracy of 95% was considered as the degree of significance of the terms. Accordingly, terms with P-values less than 0.05 are known as significant terms and were applied in the model and other terms were insignificant and removed from the model to increase the accuracy of the model. It is clear from the ANOVA tables that the P-value of the model for AP%, $K_G a_e$ and N_A was less than 0.0001, which shows the validity of the model in predicting these three responses. Furthermore, according to the p-values it can be found that for $K_G a_e$ the coded terms A, B, C, AC, AB, BC, B^2, C^2, for AP% the terms A, B, C, BC, B^2, C^2 and for N_A the terms A, B, C, AB, BC, B^2, and C^2 are significant. And by placing in Eq. (19), the following equations can predict the responses:

$$K_G a_e = +0.1369 + 0.0116A + 0.0689B - 0.0112C + 0.0079AB - 0.0048AC - 0.0129BC - 0.0397B^2 - 0.0126C^2 \quad (20)$$

$$AP = +83.77 + 2.85A + 31.68B - 8.51C - 3.12BC - 26.87B^2 - 3.04C^2 \quad (21)$$

$$N_A = +3.24 - 0.1311A + 1.19B + 0.2773C - 0.1189AB + 0.1742BC - 1.03B^2 - 0.2037C^2 \quad (22)$$

Fig. 2 shows the graph of the predicted values versus the experimental values for AP%, $K_G a_e$, and N_A. The vicinity of the points around the diagonal line indicates the high correlation between the predicted and experimental responses. The values of R^2, adjusted R^2 and predicted R^2 for AP%, $K_G a_e$, and N_A are collected in Table 5. The value of R^2 for all three responses is greater than 99%, which indicates acceptable consistency between experimental and predicted data, thus, the accuracy and validity of the model. The predicted R^2 has a reasonable prediction of the data because its

Table 5. The result of model validation for responses

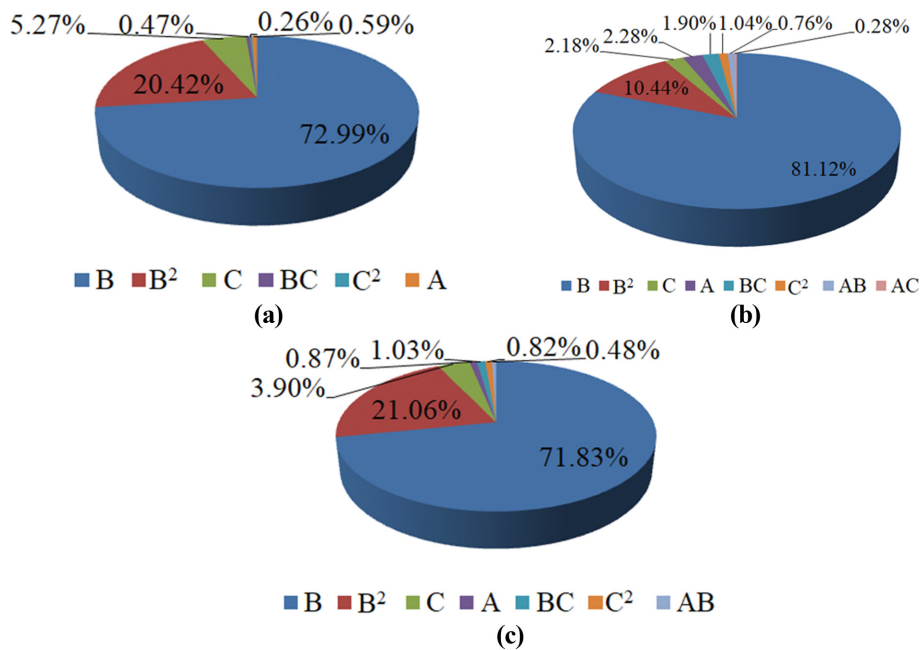|	$K_G a_e$	AP	N_A
R^2	0.9910	0.9951	0.9929
Std. Dev.	0.0068	2.31	0.1080
Adjusted R^2	0.9875	0.9939	0.9907
Mean	0.1055	65.82	2.49
Predicted R^2	0.9785	0.9916	0.9868
C.V.%	6.46	3.51	4.33
Adep precision	52.6106	77.0621	57.2719

Fig. 3. Contribution of each parameter on (a) AP, (b) K_Ga_e, and (c) N_A.

difference with adjusted R^2 is less than 0.2. The obtained adequate precision that determines the signal to noise ratio, for all three responses, is more than 4, which indicates a suitable signal for model recognition. To obtain the contribution of each parameter on the specified responses, the percentage of participation, which is defined as the sum of squares of each term to the total sum of squares, must be calculated [31]. Fig. 3 shows the share of each parameter on AP%, K_Ga_e, and N_A. According to the figure, the order of importance of the parameters for K_Ga_e is $B>B^2>A>C>BC>C^2>AB> AC$, for AP% is $B>B^2>C>A>BC>C^2$ and for N_A is as $B>B^2>C> BC>A>C^2>AB$. Statistical analysis of the results showed that the ammonia concentration with 72.99%, 71.83, and 81.12% has the greatest effect on AP%, N_A, and K_Ga_e, respectively. Then, gas flow rate with 5.27% and 3.90%, has a great effect on AP% and K_Ga_e, respectively.

3. Effect of Main Variables

3-1. TEA Concentration

Fig. 4 shows the effect of TEA concentration in the range of 10-30 wt% on the AP% and K_Ga_e. As is clear from the figure, if other variables (gas flow rate and ammonia concentration) are constant in their intermediate values, increasing the concentration of TEA
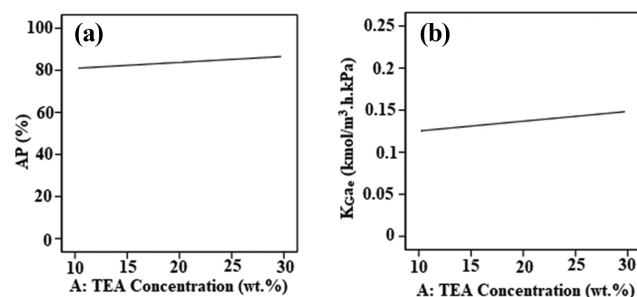

Fig. 4. Effect of TEA concentration on (a) AP, (b) K_Ga_e.

in the mentioned range improves the absorption percentage and the overall volumetric mass transfer coefficient from 81.12 to 86.53% and from 0.12 to 0.15 kmol/m³·h·kPa, respectively. There are several reasons to justify the positive correlation between TEA concentration with AP% and K_Ga_e; the absorption process of CO_2 by amine solutions is usually dependent on the liquid mass transfer in the packed column. Thus, the overall volumetric mass transfer coefficient can be expressed as $\frac{1}{K_Ga_e} \cong \frac{H}{Ek_La_e}$, where, H is Henry's constant and E is the enhancement factor. Increasing the TEA concentration in the solvent increases the number of TEA molecules as active sites per unit volume of solution to react with CO_2, which finally is associated with an increase in the chemical absorption. Increasing the TEA concentration increases the enhancement factor (E) and, as a result, decreases the mass transfer resistance of the liquid phase [25,32-35].

Furthermore, according to the preliminary tests, at high concentrations of TEA in the solvent (30-60 wt%), the viscosity also rises, which is considered an adverse factor on absorption. Since increasing the viscosity increases the mass transfer resistance of the liquid phase, this leads to a reduction in CO_2 uptake rate. Therefore, it is necessary to pay attention to the TEA concentration increase in the solvent [33].

3-2. Gas Flow

Fig. 5 shows the effect of gas flow in the range of 1,500-2,500 ml/min on the AP% and N_A. As can be seen, if the other variables (TEA concentration and ammonia concentration) are constant in their intermediate values, increasing the gas flow rate in the mentioned range reduces the absorption percentage from 90.96 to 69% and increases the mass transfer flux from 2.65 to 3.34 kmol/m²·h. The CO_2 absorption percentage decline in high gas flow rate can be expressed because by increasing the input gas flow rate, gas velocity increases. The gas velocity enhancement is associated with reduc-
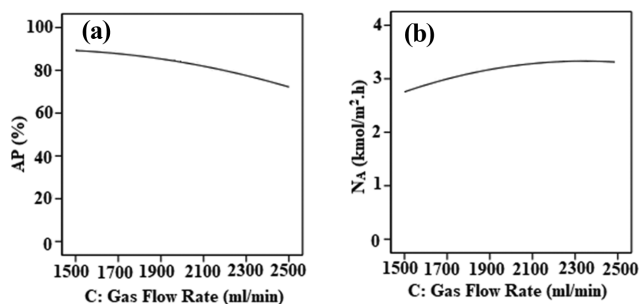
Fig. 5. Effect of gas flow rate on (a) AP, (b) N_A.

Fig. 7. Effect of AB interaction on K_Ga_e.

tion of gas phase residence time and thus increasing the CO_2 concentration at the outlet of absorption column. Therefore, by increasing the gas flow, the number of CO_2 molecules in the inlet and outlet increases, which finally, according to Eq. (11), leads to a decrease in the CO_2 absorption percentage [10,36].

Moreover, increasing the gas flow rate increases the CO_2 partial pressure through the bed, which is a desirable parameter in increasing the mass transfer flux. On the other hand, Eq. (11) shows the direct relationship between the gas flow rate and the mass transfer flux. This positive correlation is obvious in Fig. 5(b).

3-3. Ammonia Concentration

TEA is a tertiary alkanolamine which reacts slowly with CO_2. Therefore, the addition of NH_3 to aqueous TEA solution improves the reaction rate. Effect of ammonia concentration on AP%, K_Ga_e, and N_A is shown in Fig. 6. To investigate effect of ammonia concentration in the range of 0-5 wt% on the above responses, other parameters were adjusted at their intermediate values. It is clearly seen in Fig. 6(b) that with increasing concentration of ammonia, K_Ga_e increases significantly. There are several reasons to explain this observation. Raising NH_3 concentration raises the interaction between ammonia and CO_2 molecules, which thus improves the CO_2 absorption rate [37]. Increasing the concentration of ammonia leads to increasing the enhancement factor. The enhancement factor is defined as the ratio of the mass transfer coefficient of liquid film for chemical absorption to the mass transfer coefficient of liquid film for physical absorption. Increasing the concentration of ammonia causes more ammonia to be available to absorb CO_2 [38]. Ammonia improves the rate of mass transfer and affects the driving force of mass transfer [39]. Furthermore, added ammonia acts as a pH buffer, keeping high pH as CO_2 is absorbed [23].

Figs. 6(a), (c) show that increasing the NH_3 concentration in the

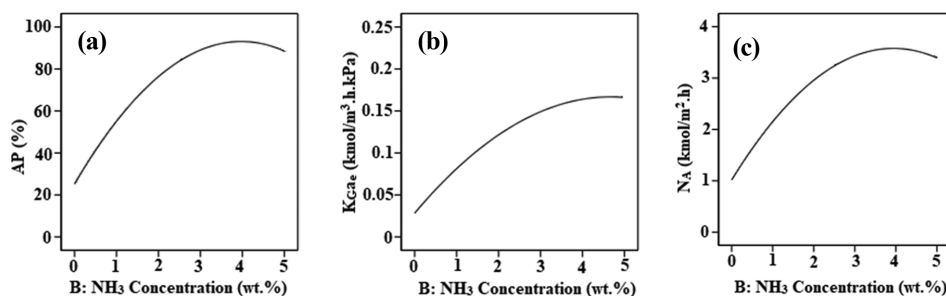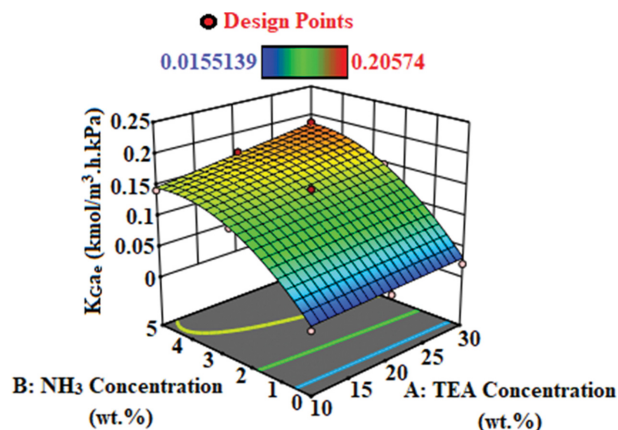range of 1-3.5 wt% leads to an increase, and in the range of 3.5-5 wt% leads to a decrease in absorption percentage and mass transfer flux. Therefore, in the range of 1-3.5 wt%, with increasing ammonia concentration, the absorption capacity of the liquid phase increases, but at higher concentrations (3.5-5 wt%), volatility and ammonia stripping prevent the physical solubility of CO_2 in the aqueous phase, which has been associated with a decrease in the absorption percentage and mass transfer flux [37,40]. Note that at high concentrations of ammonia, the viscosity also increases, which has an adverse effect on CO_2 absorption rate.

4. Interaction Between Variables

Figs. 7 and 8 show the three-dimensional diagrams related to effect of significant interactions on absorption percentage, mass transfer flux and mass transfer coefficient. Several ranges are provided to determine the number of responses that blue and red areas represent the minimum and maximum values of the responses, respectively. In examining the interaction effect between the two variables, the third variable is set at its intermediate level.

Fig. 7 shows the effect of AB interaction on mass transfer coefficient. As can be seen, the maximum amount of mass transfer coefficient is obtained at high concentrations of ammonia and TEA. The effect of TEA concentration on K_Ga_e in the absence of ammonia is slight, but in high concentrations of ammonia, increasing the concentration of TEA significantly improves K_Ga_e.

A three-dimensional chart related to the simultaneous effect of ammonia concentration and gas flow on absorption percentage, mass transfer flux and mass transfer coefficient is shown in Fig. 8.
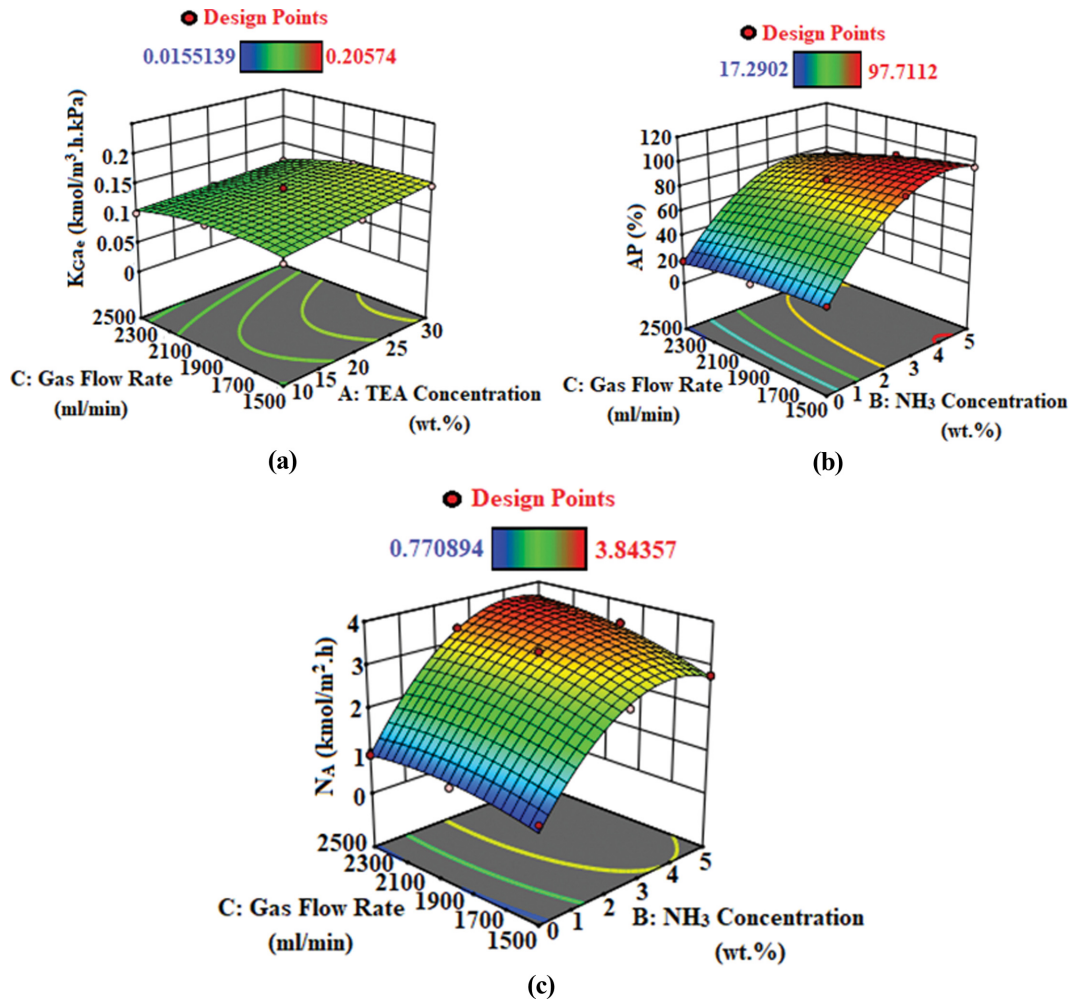

Fig. 6. Effect NH_3 concentration of (a) AP, (b) K_Ga_e, and (c) N_A.

(a)

(b)

(c)

Fig. 8. Effect of BC interaction on (a) K_Ga_e, (b) AP, (c) N_A.

Table 6. The optimal operating conditions

Variables	Unit	Optimum condition		
		AP	K_Ga_e	N_A
TEA concentration	wt%	26.68	30	11.95
NH$_3$ concentration	wt%	3.53	5	3.90
Gas flow	ml/min	1,699.46	1500	2,332.02
Optimum response	-	98.94%	0.202 kmol/m^3·h·kPa	3.901 kmol/m^2·h

It is clear that with increasing ammonia concentration to 5 wt% and decreasing gas flow to 1,500 ml/min, AP% and K_Ga_e increase to 97.71% and 0.2057 kmol/m^3·h·kPa, respectively. Also, with increasing ammonia concentration up to 5 wt% and gas flow rate up to 2,500 ml/min, the mass transfer flux reaches 3.8436 kmol/m^2·h.

OPTIMIZATION

In this study, the optimization method developed by Derringer and Suich has been used to determine the optimal operating conditions [41]. Table 6 shows the optimal operating conditions for achieving the maximum value of AP%, K_Ga_e, and N_A. As can be seen, the maximum amount of AP% (98.94%) was predicted in ammonia concentration 3.53 wt%, TEA concentration 26.68 wt%, gas flow rate 1,699.46 ml/min, and the maximum amount of overall volumetric mass transfer coefficient (0.202 kmol/m^3·h·kPa) in ammonia concentration of 5 wt%, TEA concentration 30 wt%, and gas flow rate 1,500 ml/min. The obtained mass transfer coefficient was compared with K_Ga_e of other mass transfer devices. According to the significance of ammonia concentration in this study, we focused on the research that applied ammonia for CO_2 capture. The literature survey reveals that the order of magnitude of the overall mass transfer coefficient of TEA-NH$_3$ in this study and aqueous ammonia in packed column, spray tower, and bubble column were

the same [38,42,43]. Moreover, the maximum amount of mass transfer flux (3.901 kmol/m^2·h) was obtained in ammonia concentration 3.90 wt%, TEA concentration 11.95 wt%, gas flow rate 2,332.02 ml/min. To show the superiority of the CO_2 absorption performance of the aqueous solution of ammonia-promoted TEA, the optimum absorption percentage (98.94%) was compared with the case of using only TEA and ammonia. The aqueous solution of TEA, in the mentioned condition, absorbed 30.84% of CO_2 and the AP of aqueous ammonia was 91.48%.

CONCLUSION

CO_2 absorption by ammonia added triethanolamine aqueous solution was investigated in terms of absorption percentage (AP%), overall volumetric mass transfer coefficient (K_Ga_e) and mass transfer flux (N_A) in the packed column. Three variables of ammonia concentration (0-5 wt%), TEA concentration (10-30 wt%), and gas flow (1,500-2,500 ml/min) were considered as significant variables on absorption performance. For statistical analysis of the results, the response surface three level factorial method was used.

Statistical analysis of the results showed that an ammonia concentration of 72.99%, 71.83, and 81.12% has the greatest effect on AP%, N_A, and K_Ga_e, respectively. Then, gas flow with 5.27% and 3.90%, has great effect on AP% and K_Ga_e, respectively. Thus, the addition of ammonia increases the mass transfer performance of TEA solution because it is associated with an increase in free ammonia in the solvent. The parameters for K_Ga_e as B>B^2>A>C>BC>C^2>AB>AC, for AP% as B>B^2>C>A>BC>C^2 and for N_A as B>B^2>C>BC>A>C^2>AB were obtained. Also, under optimal operating conditions, the maximum values for AP%, K_Ga_e and N_A were determined as 98.94%, 0.202 kmol/m^3·h·kPa and 3.901 kmol/m^2·h, respectively. Thus, adding ammonia to TEA improves the mass transfer performance of solvent, considerably.

ACKNOWLEDGEMENT

SUPPORTING INFORMATION

Additional information as noted in the text. This information is available via the Internet at http://www.springer.com/chemistry/journal/11814.

REFERENCES

1. Working Group II to the Fourth Assessment Report of the Intergovernmental Panel, Climate Change 2007: Impacts, Adaptation and Vulnerability, Cambridge University Press, Cambridge, United Kingdom and New York, NY, USA (2007).
2. J.-G. Lu, M.-d. Cheng, J. Yan and H. Zhang, *J. Fuel Chem. Technol.*, **37**, 740 (2009).
3. Intergovernmental Panel on Climate Working Group 1, Scientific Assessment of Climate Change, Cambridge University Press, Cambridge, Great Britain, New York, NY, USA and Melbourne, Australia (1990).
4. H. Yang, Z. Xu, M. Fan, R. Gupta, R. B. Slimane, A. E. Bland and I. Wright, *J. Environ. Sci.*, **20**, 14 (2008).
5. S. Hasanizadeh and P. Valeh-e-Sheyda, *Environ. Prog. Sustain. Energy*, **41**, e13788 (2022).
6. A. Houshmand, M. S. Shafeeyan, A. Arami-Niya and W. M. A. W. Daud, *J. Taiwan Inst. Chem.*, **44**, 774 (2013).
7. M. S. Shafeeyan, W. M. A. W. Daud, A. Shamiri and N. Aghamohammadi, *Chem. Eng. Res. Des.*, **104**, 42 (2015).
8. P. Valeh-e-Sheyda and A. Afshari, *Process Saf. Environ. Prot.*, **127**, 125 (2019).
9. H. Pashaei and A. Ghaemi, *Iran. J. Chem. Chem. Eng.*, **41**, 2771 (2021).
10. P. Valeh-e-Sheyda and J. Barati, *Process Saf. Environ. Prot.*, **146**, 54 (2021).
11. M. Akbari and P. Valeh-e-Sheyda, *Process Saf. Environ. Prot.*, **132**, 116 (2019).
12. P. Valeh-e-Sheyda, M. Faridi Masouleh and P. Zarei-Kia, *Fluid Phase Equilib.*, **546**, 113136 (2021).
13. S. Maneshdavi, S. M. Peyghambarzadeh, S. Sayyahi and S. Azizi, *J. Chem. Pet. Eng.*, **54**, 57 (2020).
14. P. Valeh-e-Sheyda and H. Rashidi, *Appl. Therm. Eng.*, **98**, 1241 (2016).
15. M. D. La Rubia, R. Pacheco, A. Sánchez, A. B. L. García, S. Sánchez and F. Camacho, *Int. J. Chem. React. Eng.*, **10**, 1 (2012).
16. M.-K. Kang, S.-B. Jeon, M.-H. Lee and K.-J. Oh, *Korean J. Chem. Eng.*, **30**, 1171 (2013).
17. S. Sarlak and P. Valeh-e-Sheyda, *Energy*, **239**, 122349 (2022).
18. F. Li, A. Hemmati and H. Rashidi, *Process Saf. Environ. Prot.*, **142**, 83 (2020).
19. A. Singh, Y. Sharma, Y. Wupardrasta and K. Desai, *Resour. Efficient Technol.*, **2**, S165 (2016).
20. S.-H. Yeon, B. Sea, Y.-I. Park, K.-S. Lee and K.-H. Lee, *Sep. Sci. Technol.*, **39**(14), 3281 (2004).
21. G. Qi, S. Wang, H. Yu, P. Feron and C. Chen, *Energy Procedia*, **37**, 1968 (2013).
22. P. S. Nair and P. Selvi, *Int. J. Sci. Res. Publication*, **4**, 1 (2014).
23. S.-B. Jeon, H.-D. Lee, M.-K. Kang, J.-H. Cho, J.-B. Seo and K.-J. Oh, *J. Taiwan Inst. Chem.*, **44**, 1003 (2013).
24. S.-W. Park, B.-S. Choi and J.-W. Lee, *Korean J. Chem. Eng.*, **23**, 138 (2006).
25. Q. Zeng, Y. Guo, Z. Niu and W. Lin, *Ind. Eng. Chem. Res.*, **50**, 10168 (2011).
26. R. Billet and M. Schultes, *Chem. Eng. Res. Des.*, **77**, 498 (1999).
27. A. A. Khan, G. Halder and A. Saha, *Int. J. Greenh. Gas Control.*, **32**, 15 (2015).
28. A. Rezaei, P. Pakzad, M. Mofarahi, A. A. Izadpanah, M. Afkhamipour and C.-H. Lee, *J. Chem. Eng. Data*, **66**, 2942 (2021).
29. M. K. Kang, S. B. Jeon, M. H. Lee and K. J. Oh, *Korean J. Chem. Eng.*, **30**, 1171 (2013).
30. A. Hemmati and H. Rashidi, *Process Saf. Environ. Prot.*, **121**, 77 (2019).
31. D. C. Montgomery, *Design and analysis of experiments*, John Wiley & Sons (2017).
32. K. Fu, T. Sema, Z. Liang, H. Liu, Y. Na, H. Shi, R. Idem and P. Tonti-

wachwuthikul, *Ind. Eng. Chem. Res.*, **51**, 12058 (2012).

33. H. Rashidi and S. Sahraie, *Energy*, **221**, 119799 (2021).

34. L. Tan, A. Shariff, K. Lau and M. Bustam, *J. Ind. Eng. Chem.*, **18**, 1874 (2012).

35. F. Wei, Y. He, P. Xue, Y. Yao, C. Shi and P. Cui, *Ind. Eng. Chem. Res.*, **53**, 4462 (2014).

36. S. Sahraie, H. Rashidi and P. Valeh-e-Sheyda, *Process Saf. Environ. Prot.*, **122**, 161 (2019).

37. N. Kittiampon, A. Kaewchada and A. Jaree, *Int. J. Greenh. Gas Control.*, **63**, 431 (2017).

38. S. Ma, B. Zang, H. Song, G. Chen and J. Yang, *Int. J. Heat Mass Transf.*, **67**, 696 (2013).

39. F. Chu, Y. Liu, L. Yang, X. Du and Y. Yang, *Appl. Energy*, **205**, 1596 (2017).

40. P. Asgarifard, M. Rahimi and N. Tafreshi, *Can. J. Chem. Eng.*, **99**, 601 (2021).

41. G. Derringer and R. Suich, *J. Qual. Technol.*, **12**, 214 (1980).

42. Q. Zeng, Y. Guo, Z. Niu and W. Lin, *Fuel Process. Technol.*, **108**, 76 (2013).

43. S. Ma, G. Chen, S. Zhu, T. Han and W. Yu, *Appl. Energy*, **162**, 354 (2016).